Dynamic Nuclear Spin Polarization in the Resonant Laser Excitation
of an InGaAs Quantum Dot

A. Högele,[1] M. Kroner,[2] C. Latta,[2,3] M. Claassen,[4] I. Carusotto,[5] C. Bulutay,[2,6] and A. Imamoglu[2]

[1]*Fakultät für Physik and CeNS, Ludwig-Maximilians-Universität München, D-80539 München, Germany*
[2]*Institute of Quantum Electronics, ETH Zürich, CH-8093, Zürich, Switzerland*
[3]*Physics Department, Harvard University, 17 Oxford Street, Cambridge, Massachusetts 02138, USA*
[4]*Department of Applied Physics, Stanford University, Stanford, California 94305, USA*
[5]*INO-CNR BEC Center and Dipartimento di Fisica, Università di Trento, I-38123 Povo, Italy*
[6]*Department of Physics, Bilkent University, Ankara, 06800, Turkey*

Resonant optical excitation of lowest-energy excitonic transitions in self-assembled quantum dots leads to nuclear spin polarization that is qualitatively different from the well-known optical orientation phenomena. By carrying out a comprehensive set of experiments, we demonstrate that nuclear spin polarization manifests itself in quantum dots subjected to finite external magnetic field as locking of the higher energy Zeeman transition to the driving laser field, as well as the avoidance of the resonance condition for the lower energy Zeeman branch. We interpret our findings on the basis of dynamic nuclear spin polarization originating from noncollinear hyperfine interaction and find excellent agreement between experiment and theory. Our results provide evidence for the significance of noncollinear hyperfine processes not only for nuclear spin diffusion and decay, but also for buildup dynamics of nuclear spin polarization in a coupled electron-nuclear spin system.

The basic principles of optical nuclear spin orientation in solids have been studied extensively in bulk semiconductors [1] and attracted revived attention by recent optical studies of semiconductor quantum dots (QDs). Dynamic nuclear spin polarization (DNSP) in self-assembled InGaAs QDs has been reported for quasiresonant [2] and nonresonant excitation [3,4]. On the basis of these experiments and related theoretical studies, a comprehensive picture of unidirectional optical orientation of QD nuclear spins effected by light-polarization selective pumping was developed. Early experiments carried out on positive and negative trions [2–4] as well as neutral excitons [5] had been used to demonstrate bistability of DNSP as a function of magnetic field or incident laser power and polarization [3,4,6,7], and to study nuclear spin buildup and decay dynamics [8,9]. In stark contrast to nonresonant excitation however, bidirectional nuclear spin orientation independent of photon polarization was observed in resonant laser scattering of elementary transitions in neutral [10] and negatively charged QDs [10–12]. A particularly striking feature of resonant DNSP using the higher energy Zeeman transition at external magnetic fields exceeding 1 T is the flattop absorption spectra, stemming from active locking of the QD resonance to the laser frequency [10,11]. Remarkably, neutral and negatively charged QDs showed similar spectral signatures in resonant spectroscopy despite substantially different energy level diagrams: for both charge states, the locking of the coupled electron-nuclear spin system to the incident laser (dragging) was observed over tens of μeV detunings to either side of the resonance [10].

In this Letter, we carry out a comprehensive experimental and theoretical analysis of dragging in resonantly driven QD transitions. We develop a microscopic model based on the effective noncollinear hyperfine coupling that was first proposed in Ref. [13] to explain nuclear spin relaxation in self-assembled QDs. Our experiments demonstrate that the nature of resonant DNSP depends drastically on whether the blue (higher energy) or the red (lower energy) Zeeman transition is resonantly excited; while the blue transition exhibits locking of the QD resonance to the incident laser, nuclear spin polarization ensures that the resonance condition is avoided for the red transition [14]. We also find that while the frequency range over which blue Zeeman transition locking takes place varies from QD to QD, the dependence of the corresponding dragging width on laser power, scan speed, and the magnetic field is similar for all QDs. A key requirement for dragging is the presence of an unpaired electron spin with a long spin-flip-time, either in the initial or the final state of the optical transition; this condition is satisfied by fundamental neutral (X^0), single-electron (X^-), and single-hole (X^+) charged QD transitions. The Overhauser field [1] experienced by this unpaired electron facilitates the feedback that modifies the QD transition energy. However, whether or not this feedback leads to *resonance seeking* (as in the blue Zeeman branch) or *resonance avoiding* (as in the red Zeeman branch) excitations depends on the spin orientation of the electron that couples to the incident laser field.

We studied individual InGaAs QDs embedded in a field effect device [15]. Two samples distinct by the thickness of the tunnel barrier between the heavily n-doped back contact and the QD layer (25 nm and 35 nm in samples A and B, respectively) were employed to probe the fundamental exciton transitions in resonant laser scattering experiments at 4.2 K [16]. Representative spectra measured on the neutral exciton X^0 in sample A subjected to a moderate magnetic field of $B_z = 4.5$ T are shown in the upper panels of Fig. 1(c) and 1(d). The spectra reveal drastic departures from a two-level Lorentzian with resonance frequency ω_X. The blue Zeeman optical transition of X^0 shows flattop absorption [Fig. 1(c)], also reported earlier for the negative trion in Faraday [10] and Voigt [11] configurations, as it is locked to the laser at frequency ω_L and can be dragged to positive and negative laser detunings $\Delta = \omega_X - \omega_L$ by tens of μeV, dependent on the scan direction [gray and blue spectra in Fig. 1(c)]. In contrast, the red Zeeman

transition avoids the resonance with the laser using DNSP [Fig. 1(d)], resulting in a triangular line shape with maximum contrast that is a factor of ~ 10 lower than its blue counterpart. We systematically measure the same qualitative response for the blue (red) Zeeman transitions of X^0 as well as of both trions, X^+ and X^-, in Faraday and Voigt magnetic field geometries, as demonstrated in Fig. 2. There are, however, quantitative variations in the efficiency of DNSP from sample to sample and even from dot to dot within one sample [17]. The thickness of the tunnel barriers in samples A and B plays a crucial role for electron-spin exchange with the Fermi reservoir via cotunneling [18] and thus for electron-spin pumping at magnetic fields exceeding ≈ 0.3 T [19] as well as the efficiency of DNSP [10].

Our findings demonstrate that effects of bidirectional DNSP are omnipresent in resonant laser spectroscopy of QD excitons and call for a unified explanation that goes
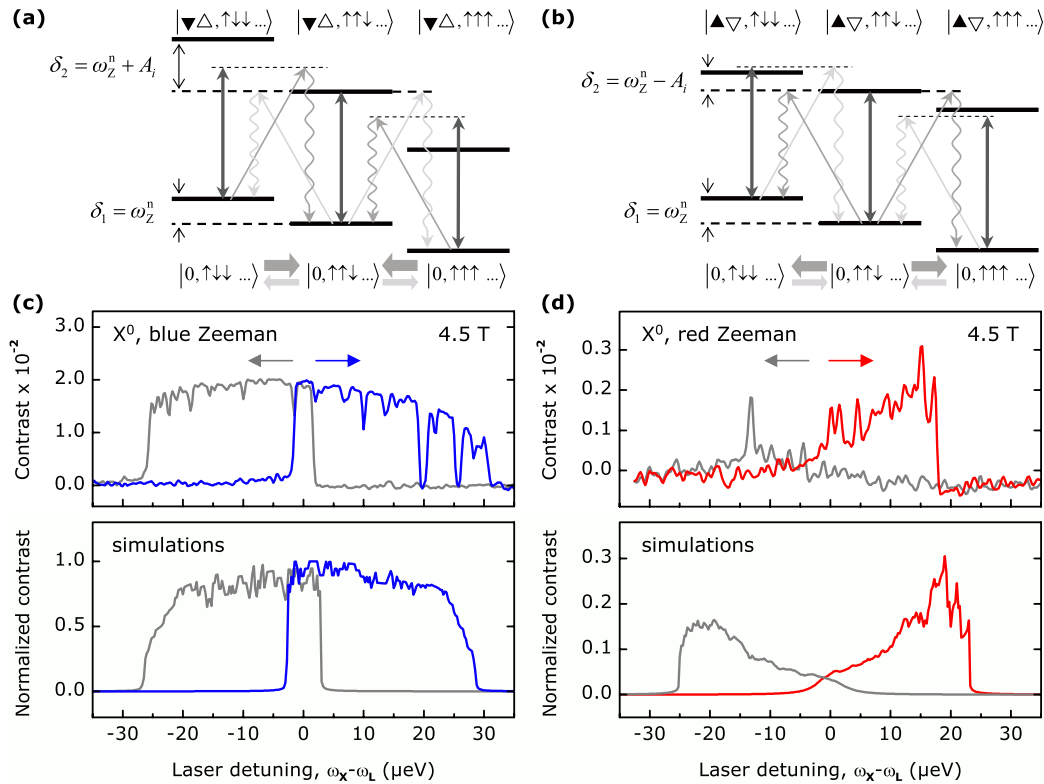

FIG. 1 (color online).   Level diagrams of the blue (a) and red (b) Zeeman transitions of a neutral exciton X^0 in a finite magnetic field applied along the growth direction z: resonant laser field couples dipole allowed and dipole forbidden transitions (straight and diagonal arrows, respectively) of the exciton-nuclear spin manifold. For both Zeeman branches the lower states of the manifold are electron-hole spin singlets $|0\rangle$ split by the nuclear spin Zeeman energy $\delta_1 = \omega_Z^n$ according to their nuclear spin orientation along z, e.g., $|\uparrow\downarrow\downarrow\ldots\rangle$ vs $|\uparrow\uparrow\downarrow\ldots\rangle$. The upper states carry both electron and hole spin excitations (full and open triangles, respectively) and sense the nuclear field of N nuclei via the Overhauser shift $\pm(A/N)$ with the electron hyperfine coupling constant A. Change in the nuclear spin polarization occurs through spin-flip assisted diagonal transitions followed by spin preserving radiative decay (wavy arrows): finite laser detunings lead to an imbalanced competition between the bidirectional nuclear spin diffusion processes within the manifold (horizontal arrows). The coupled exciton-nuclear spin system reaches steady state by locking the blue Zeeman transition to the laser (dragging) or, alternatively, pushing the red Zeeman transition away from the laser resonance (antidragging). The corresponding spectra for opposite scan directions are color-coded in (c) and (d) as gray and blue/red for initial red and blue laser detunings (upper panel: experiments on sample A, lower panel: simulations).
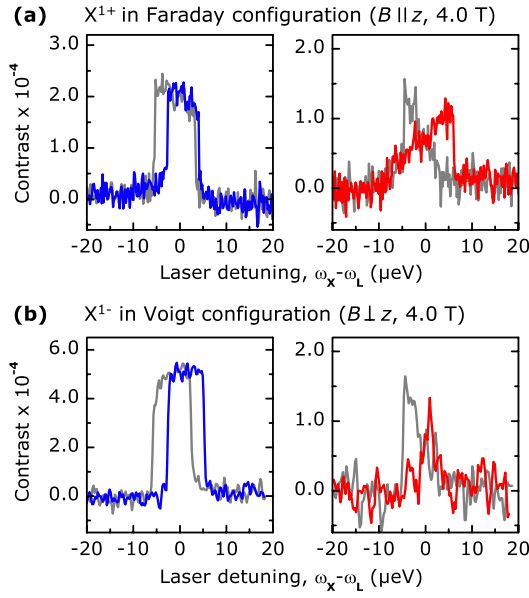
FIG. 2 (color online). Optical transitions in quantum dots of sample *B* at $B = 4.0$ T as a function of quantum dot charge and magnetic field orientation: positive and negative trions, X^+ and X^-, exhibit characteristic flattop resonances on the blue Zeeman transition and triangular line shapes on the red Zeeman transition (left and right panels in *a* and *b*, respectively) in magnetic field oriented (a) parallel (Faraday) and (b) perpendicular (Voigt) to the sample growth axis *z*.

beyond directional DNSP mediated by flip-flop terms of the Fermi-contact hyperfine interaction. Obviously, the model should be insensitive to the details of the initial and final QD states, such as charge configuration or the presence of dark exciton states [20], yet capture marked signatures and differences in the response of the blue and red Zeeman transitions to a near-resonant laser. Recently, Yang and Sham [14] proposed that noncollinear hyperfine interaction between heavy-holes and the nuclei, induced by heavy-light-hole coupling, provides an excellent qualitative description of the signatures related to DNSP in resonant laser scattering [21]. On the other hand, recent experiments [22] demonstrate that noncollinear hyperfine interaction between the electron and the nuclei plays a significant role in determining QD nuclear spin dynamics even in the absence of optically generated holes; this interaction is induced by large quadrupolar fields in strained self-assembled QDs which ensure that nuclear spin projection along B_z is not a good quantum number. The resulting effective noncollinear interaction between the QD electron and the nuclei is [13]:

$$\hat{H}_{nc} = \sum_i A_i^{nc} \hat{I}_x^i \hat{S}_z. \quad (1)$$

A key result of this Letter is the demonstration that $\hat{H}_{nc}$ provides an excellent quantitative explanation of the resonance seeking and avoiding effects observed in resonant DNSP. In Eq. (1), $A_i^{nc} = A_i B_Q^i \sin(2\theta_i)/\omega_Z^n$, and $\hat{S}$, $\hat{I}^i$, spin

operators of the electron spin and the *i*th nucleus, respectively. ω_Z^n denotes the nuclear Zeeman energy, B_Q^i the strength of the quadrupolar interaction, and θ_i is the angle between the major quadrupolar axis of the *i*th nucleus and the *z*-axis. For the coupling strength of the electron to the *i*th nucleus we assumed $A_i = A/N$, where A is the hyperfine coupling constant and N the number of nuclei. To determine B_Q^i and θ_i, we first employed molecular statics with Tersoff type force fields [23] to obtain the realistic structure for more than 1×10^6 atoms hosting $N \simeq 32\,000$ QD nuclei. The atomistic strain and nuclear quadrupolar distributions are extracted over this relaxed structure [24]. Figure 3(a) shows the distribution of the biaxial strain $\epsilon_B \equiv \epsilon_{zz} - (\epsilon_{xx} + \epsilon_{yy})/2$ which is primarily responsible for the nuclear quadrupolar shifts. Based on this distribution, we determine A_i^{nc} for a line cut along the QD taken through the center and the [010] axis cf. Fig. 3(b). Averaging over this distribution for nuclei that lie within the Gaussian QD electron wave function, we obtain $A_i^{nc} \simeq 2.6 \times 10^{-4}$ μeV, consistent with [22].

The fact that $\hat{H}_{nc}$ could explain dragging is at first sight surprising since its dominant effect appears to be nuclear spin diffusion. However, a careful inspection shows that the same Hamiltonian also leads to a small polarization term whose direction is determined by the sign of the optical detuning [14,17]. To explain this, we consider the energy-level diagrams of X^0 in Fig. 1(a) and 1(b), each showing a ladder of two-level quantum systems coupled by nuclear spin-flip processes. Here we adopt a mean-field
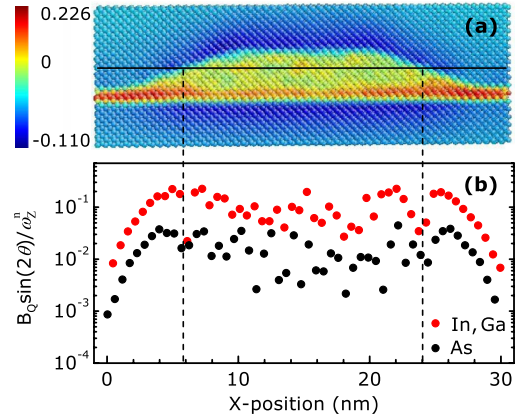

FIG. 3 (color online). (a) Distribution of the biaxial strain ϵ_B, which primarily controls the quadrupolar splitting, over the (100) plane bisecting a truncated coned-shaped quantum dot. The false color plot illustrates the tensile strain distribution with rapid variations within the quantum dot region arising from the random composition of the $In_{0.7}Ga_{0.3}As$ alloy used in the model. (b) The value of $B_Q^i \sin(2\theta_i)/\omega_Z^n$ evaluated over the line cut through the monolayer indicated by the solid line in (a) Averaging over this distribution with a Gaussian envelope for the electron wave function we obtain a value of 0.0124 for cations (In or Ga) and 0.0848 for anions (As).

description of the nuclear spins by neglecting the quantum fluctuations in the Overhauser field ($I_z = \langle \hat{I}_z \rangle$) and limit ourselves to effective spin 1/2 nuclei for simplicity. We consider the limit of a large external magnetic field where $\omega_Z^e \gg \omega_Z^n \gg \Omega \sim \Gamma_0$ (ω_Z^e is the electron Zeeman energy, Ω the laser Rabi frequency, and Γ_0 the radiative decay rate). In this limit, all nuclear spin-flip processes, including those described by $\hat{H}_{nc}$ are energetically forbidden to first order in perturbation theory. Using a Schrieffer-Wolff (SW) transformation, we arrive at the following correction terms to the laser-exciton coupling:

$$\hat{H}_{nc-laser} = i \sum_i \frac{\Omega A_i^{nc}}{2\omega_Z^n} [(\hat{\sigma}_{0X} - \hat{\sigma}_{X0})\hat{I}_y^i] \quad (2)$$

with $\hat{\sigma}_{0X} = |0\rangle\langle X|$. Here, $|X\rangle$ and $|0\rangle$ denote the exciton and vacuum state, respectively. Application of the same SW transformation to the Liouvillian term leads to nuclear-spin-flip assisted spontaneous emission terms with maximum rate $\simeq \Gamma_0(A_i^{nc}/4\omega_Z^n)^2$. In the limit $\omega_Z^n \sim \Gamma_0$ of interest, the denominator in Eq. (2) should be modified to take into account broadening of the excitonic spin states due to spontaneous emission. Spin-flip Raman scattering processes arising from the Fermi-contact hyperfine interaction take place at a rate $\simeq \Gamma_0(A_i/2\omega_Z^e)^2$ and are a factor ~ 100 times slower given that $\omega_Z^e \simeq 1000\,\omega_Z^n$ and $A_i^{nc} \simeq 0.02\,A_i$.

For a given nuclear spin polarization I_z, e.g., $|\uparrow\uparrow\downarrow\ldots\rangle$, we can label the two-level system by the states $|0, I_z\rangle$ and $|\blacktriangledown\triangle, I_z\rangle$. The ground states $|0, I_z\rangle$ differ by an energy $\delta_1 = \omega_Z^n$. The corresponding energy differences for the excited states are $\delta_2 = \omega_Z^n + A_i$ and $\omega_Z^n - A_i$ for the blue and red Zeeman transition, respectively. The transition rate associated with hyperfine-assisted laser coupling is given for the blue Zeeman branch [Fig. 1(a)] by [25]:

$$W_{\pm}(I_z) = \left(\frac{\Omega A_i^{nc}}{4\omega_Z^n}\right)^2 \frac{\Gamma_0}{4\delta_{\pm}^2 + \Gamma_0^2 + \Omega^2/2}. \quad (3)$$

A remarkable feature of $W_{\pm}(I_z)$ is its dependence on the sign of the laser detuning entering through the effective optical detuning $\delta_{\pm} = \Delta - A_i(I_z \pm 1) \mp \omega_Z^n$: when the incident laser field is red (blue) detuned, the transition rate $W_+(I_z)$ ($W_-(I_z)$) dominates over $W_-(I_z)$ ($W_+(I_z)$) and ensures that the Overhauser field increases (decreases). This directional DNSP will in turn result in a decrease of the effective detuning δ from $\Delta - A_i I_z$ to $\Delta - A_i(I_z + 1)$ for a red detuned laser and to $\Delta - A_i(I_z - 1)$ for a blue detuned laser. If initially $I_z \ll N/2$, then DNSP will continue until $\delta \simeq 0$.

While a laser scan across the blue transition leads to a positive feedback of the nuclear spins to ensure locking condition, a scan across the red Zeeman line causes an antidragging effect. To understand this, we note that the effective optical detuning in this case is $\delta_{\pm} = \Delta + A_i(I_z \pm 1) \mp \omega_Z^n$. The simple sign change in the effective optical detuning renders the exact resonance between the laser

field and the red exciton transition an unstable point. The DNSP that ensues in the presence of a small but nonzero δ will result in nuclear-spin-flip processes that increase $|\delta|$ and push the red Zeeman transition away from the laser resonance. The experiments validate these conclusions [Fig. 1(d) and right panel of Fig. 2].

To obtain a quantitative prediction, we consider the rate equation

$$\frac{dI_z}{dt} = W_+(I_z)\left(\frac{N}{2} - I_z\right) - W_-(I_z)\left(\frac{N}{2} + I_z\right) - \Gamma_d I_z \quad (4)$$

which includes nuclear-spin-flip assisted spontaneous emission processes leading to pure nuclear spin diffusion at rate Γ_d [17]. The steady-state solution exhibits bistability due to the nonlinear I_z dependence of the rates $W_{\pm}(I_z)$. For a given initial laser detuning Δ the solution of the rate equation yields the steady-state nuclear spin polarization I_z and thus the effective optical detuning δ as established within the integration time t_c of the experiment. The absorption spectrum is calculated by varying the laser detuning in discrete steps Δ_n. The rate equation (4) is symmetric with respect to the laser detuning. In order to account for the asymmetry observed experimentally for the two scan directions, we refined the model by including terms for spin-flip Raman scattering processes that arise from the Fermi-contact hyperfine interaction as well as an unbalanced telegraph noise in the resonance condition [17]. We find excellent agreement between theory and experiment, as demonstrated in Fig. 1.

Remarkably, the model also reproduces the dependence of DNSP in resonant laser scattering on key experimental parameters. Figure 4 shows how the dragging width evolves as a function of scan speed. Both the detuning step Δ_n and the waiting time constant t_c used for signal integration after each step contribute to the effective scan speed of the laser detuning: for a given Δ_n the maximum width increases nonlinearly with t_c. This nonlinearity
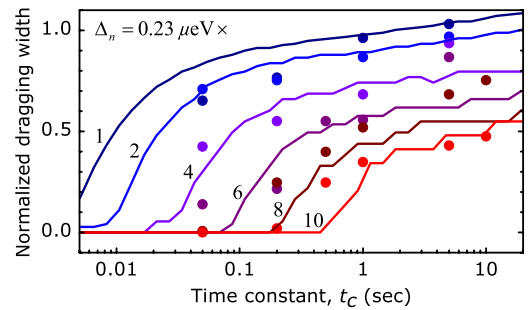

FIG. 4 (color online). The parametric plot depicts the dragging width obtained for incremental laser detuning steps $\Delta_n = n \times 0.23\,\mu eV$ from $0.23\,\mu eV$ (top, dark blue) to $2.30\,\mu eV$ (bottom, red) at different time constants (closed circles: experiments, solid lines: simulations; the parametric increment n is given in numbers, the set of data was normalized to the value of the dragging width for $n = 1$ at 5 s). The full dynamic range of the experiment is correctly reproduced by the model.

makes our simulations highly sensitive to the set of parameters that determine the DNSP dynamics; in particular, it allows us to extract a value for A_i^{nc} for a given set of N and A. Figure 4 demonstrates that the full dynamic range of the experiment is correctly captured with the following set of parameters: $\hbar\Gamma_0 = 0.7$ μeV, $\Omega = 0.5\Gamma_0$, $B = 4.5$ T, step size $\Delta_n = n \times 0.23$ μeV, $\omega_Z^e/\omega_Z^n = 1000$, $N = 3.2 \times 10^4$, $A_i = 120$ μeV$/N$, and $A_i^{nc} = 0.45 \times 10^{-4}$ μeV. The value for the noncollinear hyperfine coupling constant found from simulations is in good agreement with that obtained independently from atomistic calculations and nuclear spin decay measurements [22]. The same set of parameters was also used to reproduce the external magnetic field and the laser power dependence [17] and to calculate the absorption spectra in Fig. 1 recorded with a dwell time of $t_c = 0.2$ s.

Our results establish quadrupolar interaction induced noncollinear hyperfine coupling as the mechanism responsible for resonant bidirectional DNSP that is ubiquitous for self-assembled QDs. This finding goes beyond the traditional notion of noncollinear hyperfine processes as being responsible for nuclear spin diffusion and decay. Arising from the interplay of Fermi-contact hyperfine coupling and lattice strain, noncollinear interaction is not restricted to the specific details of the material system studied here. On the contrary, it is of general significance for the coupled electron-nuclear spin dynamics in condensed matter systems, where strain is inherent to the crystalline matrix. An obvious extension of our work will be to carry out similar experiments in materials with different strain conditions such as in interface or droplet QDs or in nitrogen vacancy centers in diamond.

[1] F. Meier and B. P. Zakharchenya, *Optical orientation* (North-Holland, Amsterdam, 1984).

[2] C. W. Lai, P. Maletinsky, A. Badolato, and A. Imamoglu, Phys. Rev. Lett. **96**, 167403 (2006).

[3] B. Eble *et al.*, Phys. Rev. B **74**, 081306 (2006).

[4] A. Tartakovskii *et al.*, Phys. Rev. Lett. **98**, 026806 (2007).

[5] T. Belhadj *et al.*, Phys. Rev. Lett. **103**, 086601 (2009).

[6] P. Maletinsky, C. W. Lai, A. Badolato, and A. Imamoglu, Phys. Rev. B **75**, 035409 (2007).

[7] P.-F. Braun *et al.*, Phys. Rev. B **74**, 245306 (2006).

[8] P. Maletinsky, A. Badolato, and A. Imamoglu, Phys. Rev. Lett. **99**, 056804 (2007).

[9] P. Maletinsky, M. Kroner, and A. Imamoglu, Nature Phys. **5**, 407 (2009).

[10] C. Latta *et al.*, Nature Phys. **5**, 758 (2009).

[11] X. Xu *et al.*, Nature (London) **459**, 1105 (2009).

[12] T. D. Ladd *et al.*, Phys. Rev. Lett. **105**, 107401 (2010).

[13] C.-W. Huang and X. Hu, Phys. Rev. B **81**, 205304 (2010).

[14] W. Yang and L. J. Sham, arXiv:1012.0060.

[15] H. Drexler, D. Leonard, W. Hansen, J. P. Kotthaus, and P. M. Petroff, Phys. Rev. Lett. **73**, 2252 (1994).

[16] A. Högele *et al.*, Phys. Rev. Lett. **93**, 217401 (2004).

[17] See Supplemental Material at http://link.aps.org/supplemental/10.1103/PhysRevLett.108.197403 for details.

[18] J. M. Smith *et al.*, Phys. Rev. Lett. **94**, 197402 (2005).

[19] M. Atatüre *et al.*, Science **312**, 551 (2006).

[20] M. Bayer *et al.*, Phys. Rev. Lett. **82**, 1748 (1999).

[21] Experimentally determined values of hole-hyperfine interaction would suggest that the resulting nuclear spin-flip rates would be an order of magnitude too small to explain the relative insignificance of the directional reverse Overhauser effect. In addition, the large apparent variation in heavy-light-hole mixing in QDs as indicated by the measured in-plane hole g-factors would suggest that dragging features would change appreciably from QD to QD, if the mechanism was due to hole-hyperfine interaction.

[22] C. Latta, A. Srivastava, and A. Imamoglu, Phys. Rev. Lett. **107**, 167401 (2011).

[23] D. Powell, M. A. Migliorato, and A. G. Cullis, Phys. Rev. B **75**, 115202 (2007).

[24] C. Bulutay, Phys. Rev. B **85**, 115313 (2012).

[25] By carrying out a complete numerical analysis, we have confirmed that the saturation of $W_{\pm}(I_z)$ is correctly taken into account in Eq. (2).